

Fate of Weyl semimetals in the presence of incommensurate potentials

Yucheng Wang¹ and Shu Chen^{1,2,3,*}

¹*Beijing National Laboratory for Condensed Matter Physics,
Institute of Physics, Chinese Academy of Sciences, Beijing 100190, China*

²*School of Physical Sciences, University of Chinese Academy of Sciences, Beijing, 100049, China*

³*Collaborative Innovation Center of Quantum Matter, Beijing, China*

We investigate the effect of the incommensurate potential on Weyl semimetal, which is proposed to be realized in ultracold atomic systems trapped in three-dimensional optical lattices. For the system without the Fermi arc, we find that the Weyl points are robust against the incommensurate potential and the system enters into a metallic phase only when the incommensurate potential strength exceeds a critical value. We unveil the transition by analysing the properties of wave functions and the density of states as a function of the incommensurate potential strength. We also study the system with Fermi arcs and find the Fermi arcs are sensitive against the incommensurate potential and can be destroyed by a weak incommensurate potential.

PACS numbers: 67.85.-d, 71.30.+h, 72.15.Rn, 71.55.Ak

I. INTRODUCTION

During the past few years, considerable attention has been paid on topological phases of matter, which include the gapped topological insulators [1, 2] and various gapless systems [3, 4]. Weyl semimetal (WSM), one prime example of these gapless systems, has been widely studied both in theories [6–12] and on the experiments [13–16]. A WSM is a three-dimensional topological semimetal which has some isolated touching points between conduction and valence bands. These touching points are called Weyl nodes and have definite chiralities, which can be understood as the topologically protected chiral charges. Weyl nodes with opposite chiralities in momentum space can be connected by nonclosed surface states, which are called Fermi arc states [6].

The effects of disorder on Weyl semimetals [17–24] and Dirac semimetals [25–28] have been a subject of intensive study. It has been found that a WSM phase or a Dirac semimetal phase is robust against weak disorder and there exist semimetal-metal-insulator quantum phase transitions when the strength of disorder increases. Some recent works [29–35] proposed to realize the Weyl Hamiltonian for ultracold atoms in three-dimensional optical lattices by using laser-assisted tunneling. On the other hand, one can generate incommensurate optical lattices by superimposing two 1D optical lattices with incommensurate wavelengths [36, 37], which has been widely applied to study the localization to delocalization transition induced by the incommensurate potential [38–46]. One interesting question is what is the fate of the WSM when adding incommensurate potential in one direction of the three-dimensional optical lattice for a Weyl Hamiltonian. To examine this question, we add an additional incommensurate potential to the proposed Weyl Hamiltonian [29] and investigate the effect of incommen-

surate potential on the WSM phase.

This paper is organized as follows: in Sec. II, we introduce the model of Weyl Hamiltonian with additional incommensurate potential added in one direction of the three-dimensional optical lattice. We firstly consider the case in the absence of Fermi arc and investigate the extended-localization transition of the system in the direction with incommensurate potential by studying the inverse participation ratio (IPR) of wave functions. By analysing the change of density of states (DOS) of this system, we demonstrate the occurrence of a transition from WSM to a two-dimensional metallic phase. We then consider the case in the presence of Fermi arcs and study the effect of incommensurate potential on the Fermi arcs. A brief summary is given in Sec. III.

II. MODEL AND RESULTS

We consider the model that can be realized for ultracold atoms in three-dimensional optical lattices [29] described by

$$H_0 = - \sum_{m,n,l} (t_x e^{-i\phi_{m,n,l}} a_{m+1,n,l}^\dagger a_{m,n,l} + t_y a_{m,n+1,l}^\dagger a_{m,n,l} + t_z e^{-i\phi_{m,n,l}} a_{m,n,l+1}^\dagger a_{m,n,l} + \text{H.c.}), \quad (1)$$

where $a_{m,n,l}$ ($a_{m,n,l}^\dagger$) is the annihilation (creation) operator on the site (m, n, l) , t_x , t_y and t_z are the hopping strengths along x , y and z directions, respectively, and $\phi_{m,n,l} = (m + n)\pi$ (modulo 2π). After applying Bloch's theorem, one can obtain the Hamiltonian in the momentum space

$$H_0(k) = -2(t_y \cos k_y \sigma_x + t_x \sin k_x \sigma_y - t_z \cos k_z \sigma_z), \quad (2)$$

where $\sigma_{x,y,z}$ are Pauli matrices and the wave vectors k_x , k_y and k_z are defined in the first Brillouin of a $L_x \times L_y \times L_z$ cubic lattice. Throughout this paper we set

*schen@iphy.ac.cn

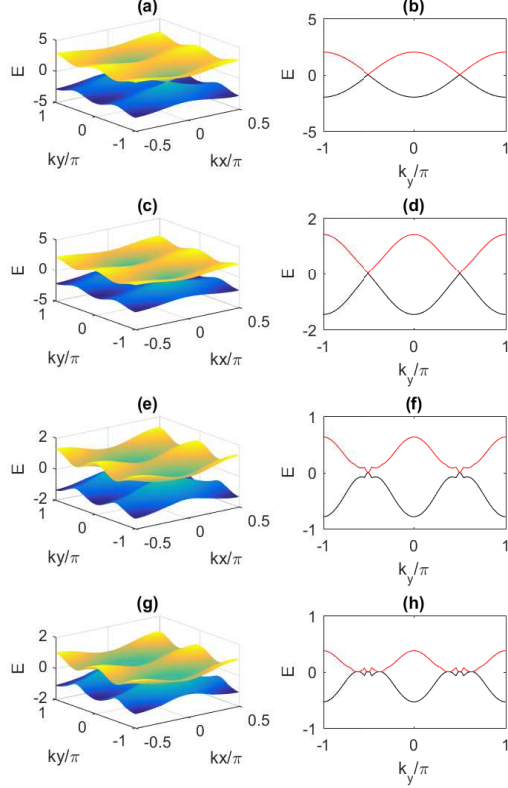


FIG. 1: (Color online) Dispersions of the L -th and $(L+1)$ -th levels of the system with (a) $V = 0$, (c) $V = 1$, (e) $V = 2.1$ and (g) $V = 2.5$ and the corresponding dispersions versus k_y with fixed $k_x = 0$ in (b), (d), (f) and (h), respectively. Here we consider the system with $L = 300$ under OBC in z direction and PBC in the x and y directions.

$L_x = L_y = L_z = L$, $t_x = t_y = t_z = 1$ and the lattice constant $a = 1$.

The energy spectrum of the Hamiltonian is given by

$$E(k) = \pm 2\sqrt{t_x^2 \sin^2(k_x) + t_y^2 \cos^2(k_y) + t_z^2 \cos^2(k_z)}, \quad (3)$$

which consists of two bands touching at four Weyl points $(k_x, k_y, k_z) = (0, \pm\pi/2, \pm\pi/2)$ [29]. If we take the open boundary conditions (OBC) along the z direction and periodic boundary conditions (PBC) in the x and y directions, k_z is no longer a good quantum number. Nevertheless, the upper and lower bands still touch at the Weyl points $(k_x, k_y) = (0, \pm\pi/2)$. To be clear, we show the energy dispersions of the L -th and $(L+1)$ -th levels in Fig. 1(a) with $L = 300$ and also in Fig. 1(b) the energy as a function of k_y by fixing $k_x = 0$. One can find that the dispersions around the two Weyl points are linear, and there exists no Fermi arc. Then we add quasiperiodic potential along the z direction and the Hamiltonian can be described by

$$H = H_0 + V \sum_l \cos(2\pi\alpha l). \quad (4)$$

where α is an irrational number chosen as $\alpha = (\sqrt{5}-1)/2$.

Since k_x and k_y are good quantum numbers with $k_x = \frac{2\pi}{L}i_x$ and $k_y = \frac{2\pi}{L}i_y$, where $i_x = -\frac{L}{4}, -\frac{L}{4}+1, \dots, \frac{L}{4}$ and $i_y = -\frac{L}{2}, -\frac{L}{2}+1, \dots, \frac{L}{2}$, we can still diagonalize the Hamiltonian (4) in the momentum space of k_x and k_y . By representing the n -th eigenstate as $|\Psi_n\rangle = [\psi_{n,1,A}, \psi_{n,1,B}, \psi_{n,2,A}, \psi_{n,2,B}, \dots, \psi_{n,L,A}, \psi_{n,L,B}]^T$ and using $H|\Psi_n\rangle = E_n|\Psi_n\rangle$, where E_n is the corresponding eigenvalue, one can obtain the following explicit forms:

$$\begin{aligned} E_n \psi_{n,j,A} &= t_z(\psi_{n,j-1,A} + \psi_{n,j+1,A}) + V \cos(2\pi\alpha j) \psi_{n,j,A} + (-2t_y \cos k_y + 2it_x \sin k_x) \psi_{n,j,B}, \\ E_n \psi_{n,j,B} &= -t_z(\psi_{n,j-1,B} + \psi_{n,j+1,B}) + (-2t_y \cos k_y - 2it_x \sin k_x) \psi_{n,j,A} + V \cos(2\pi\alpha j) \psi_{n,j,B}, \end{aligned} \quad (5)$$

where j expresses the j -th layer along the \hat{z} direction. When fixing k_x and k_y , the eigenvalue problem of the Hamiltonian (4) reduces to diagonalize a $2L \times 2L$ matrix. By solving Eq. (5), we can get the energy dispersion $E_n(k_x, k_y)$ for various V and study the change of energy spectrum. In Fig. 1(c)-(h), we present the L -th and $(L+1)$ -th level of the system with $V = 1, 2.1$ and 2.5 , respectively. While Fig. 1(c), (e), (g) show $E_n(k_x, k_y)$ versus k_x and k_y , Fig. 1(d), (f), (h) show the corresponding E_n as a function of k_y with fixed $k_x = 0$. While the Weyl points at $(k_x, k_y) = (0, \pm\pi/2)$ are not destroyed when the incommensurate potential strength is not so strong, e.g., $V = 1$ as shown in Fig. 1(c) and (d), the

spectrum structure is completely changed when $V = 2.5$, as shown in Fig. 1(g) and (h).

To investigate the extended-localization transition in the z direction, we introduce the IPR [47, 48] of the system with fixed k_x and k_y , which is defined as

$$IPR = \sum_j (\psi_{n,j,A}^2 + \psi_{n,j,B}^2)^2 \quad (6)$$

for a normalized wave function Ψ_n . The IPR is a useful quantity to characterize the delocalization-localization transition of a disorder or incommensurate system. The IPR approaches to zero in the thermodynamic limit for

an extended state, but tends to a finite value of $O(1)$ for a localized state. We further define the mean IPR as

$$MIPR = \frac{1}{2L} \sum_{n=1}^{2L} \sum_j (\psi_{n,j,A}^2 + \psi_{n,j,B}^2)^2, \quad (7)$$

which is the average of IPRs for all the eigenstates. We display the IPR of the $L - th$ eigenstate in Fig. 2(a) and the MIPR in Fig. 2(b) as a function of k_x and k_y for $V = 1.9$. It is shown that states around $(k_x, k_y) = (0, \pm\pi/2)$ are still in extended states, whereas the states in the corner and side regimes of momentum space already becomes localized in the z direction, i.e., states around $(k_x, k_y) = (0, \pm\pi/2)$ are harder to become localized than states in other regimes. In order to localize the states around the Weyl points, one needs increase the incommensurate potential strength V . This property can be further clarified from Fig. 2(c) and Fig. 2(d), which show the IPR of the $L - th$ eigenstate and MIPR as a function of k_x and V with the fixed $k_y = \frac{\pi}{2}$, respectively. Similarly, in Fig. 2(e) and Fig. 2(f), we show the IPR and MIPR as a function of k_y and V by fixing $k_x = 0$. From these figures, we see that some eigenstates become localized along the z direction when V increases over about 0.4, however states around $(k_x, k_y) = (0, \pm\pi/2)$ become localized when $V > 2$. This phenomenon can be understood from Eq. (5). The hopping strength along x or y direction is stronger, the localization in the z direction gets easier. When $k_x = 0$ and $k_y = \pm\frac{\pi}{2}$, the effective hopping strengths along the x and y directions are zero, and the model can be mapped to the one-dimensional (1D) Aubry-André (AA) model [38]. It is well known that all single particle states in the AA model are extended when $V < 2$, whereas they are localized when $V > 2$. This is consistent with our result that all eigenstates are localized along the z direction when $V > 2$.

To further see how the WSM is changed against the increasing of incommensurate potential, we calculate the DOS, which is defined as

$$\begin{aligned} \rho(E) &= \frac{1}{L^3} \sum_{i=1}^{L^3} \delta(E - E_i) \\ &= \frac{1}{L^3} \sum_{l=1}^{2L} \sum_{i_x=-\frac{L}{4}}^{\frac{L}{4}} \sum_{i_y=-\frac{L}{2}}^{\frac{L}{2}} \delta(E - E_{l,i_x,i_y}). \end{aligned} \quad (8)$$

Here E_{l,i_x,i_y} is the $l - th$ eigenstate with fixed $k_x = \frac{2\pi}{L}i_x$ and $k_y = \frac{2\pi}{L}i_y$. To numerically calculate $\delta(E - E_i)$, we make an approximation by replacing the function of $\delta(x)$ by a Gaussian function $\frac{1}{\sqrt{\pi\sigma^2}} \exp(-\frac{x^2}{\sigma^2})$, [49] which approaches the δ -function exactly when $\sigma \rightarrow 0$. The WSM is characterized by the DOS $\rho(E) \sim |E|^2$, which gives rise to $\rho(0) = 0$. On the other hand, the DOS $\rho(0)$ becomes finite if the system enters into a metallic phase. So $\rho(0)$ can give signatures of the transition from a WSM to metal phase. Fig. 3(a) gives the DOS at zero energy as a function of incommensurate potential strength for

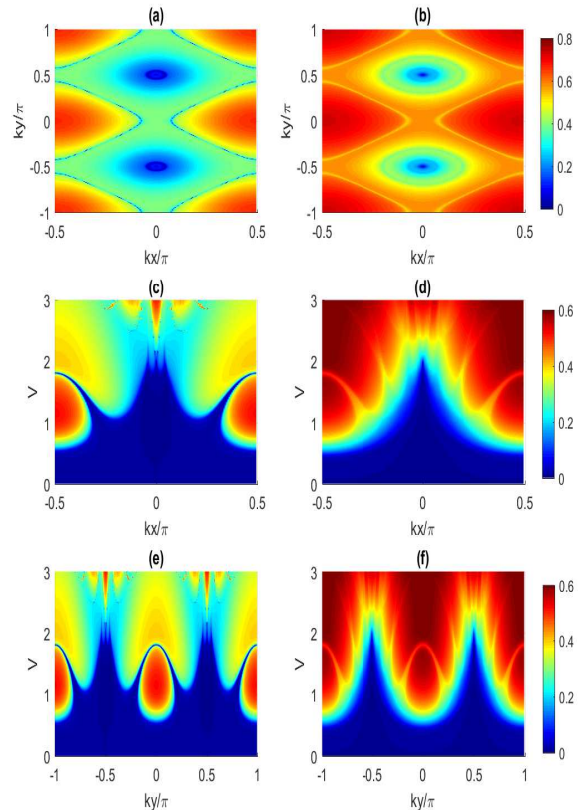


FIG. 2: (Color online) (a) IPR and (b) MIPR as a function of k_x and k_y with fixed $V = 1.9$. (c) IPR and (d) MIPR as a function of k_x and V with fixed $k_y = \frac{\pi}{2}$. (e) IPR and (f) MIPR as a function of k_y and V with fixed $k_x = 0$. The lattice size is $L = 300$.

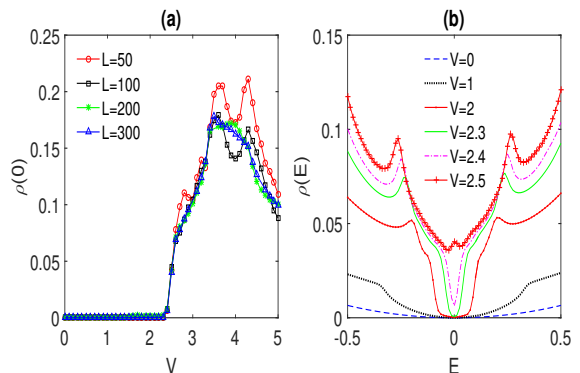


FIG. 3: (Color online) (a) $\rho(0)$ versus V for different lattice size L with fixed $\sigma = 0.02$. (b) DOS with $L = 300$ as a function of energy for various values of incommensurate potential strength V .

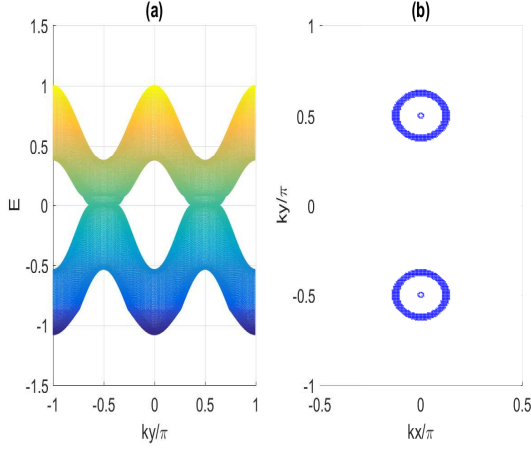


FIG. 4: (Color online) (a) The projection of dispersions of L -th and $(L+1)$ -th levels of the system with $V = 2.5$ on the $k_y - E$ plane. (b) The cross section of energy dispersion $E(k_x, k_y)$ at $E = 0 \pm 0.001$.

different L . It is shown that the transition point isn't sensitive to the lattice size when $L > 50$, so it is reliable to choose $L = 300$. From Fig. 3(a), the WSM-metal transition point can be found at about $V = 2.3$. Fig. 3(b) shows the DOS with $L = 300$ as a function of energy for various values of V . For $V = 0$, $\rho(E) \sim |E|^2$. This relation holds true in the region of $|E| \sim 0$ even in the presence of a finite V and we have $\rho(0) = 0$ as long as V is less than 2.3. Such a relation no longer holds true when V is larger than $V_c = 2.3$, as $\rho(0)$ rapidly increases and becomes finite once $V > V_c$.

The change of DOS is closely related to the change of

spectrum structure of the system. We find that the structure of the energy dispersion $E(k_x, k_y)$ does not change dramatically at $V = 2$, even all eigenstates become localized in the z direction when $V > 2$. For example, as shown in Fig. 1(e) and (f), for $V = 2.1$, the Weyl points don't disappear and the dispersion relation are still linear near the Weyl points. However, when increasing V further to exceed V_c , for example $V = 2.5$ as shown in Fig. 1(g) and Fig. 1(h), one can find the touched segment of the L -th and $(L+1)$ -th levels of this system no longer has a similar structure of Weyl points. To be clear, we show the spectrums of L -th and $(L+1)$ -th levels projected onto the $k_y - E$ plane in Fig. 4(a) and the cross section at $E = 0 \pm 0.001$ (with considering the effect size effect) in Fig. 4(b). It is clear that the two-band touched segment is no longer composed of some single points and there exist many states for $E = 0$, i.e., $\rho(0)$ becomes a finite value. Correspondingly, the system becomes a metal. In this metal phase, we note that the wave functions in the z direction are localized but the wave functions in the x and y directions are extended, i.e., the system can be viewed as a two-dimensional metal.

If we take OBC in the $\hat{x} - \hat{y}$ direction and PBC in the \hat{z} and $\hat{x} + \hat{y}$ directions, $k_{\parallel}(\hat{x} + \hat{y})$ and k_z are good quantum numbers and the Weyl points on the (k_{\parallel}, k_z) plane are at $(k_{\parallel}, k_z) = (\pm \frac{\pi}{2\sqrt{2}}, \pm \frac{\pi}{2})$, which are connected with Fermi arcs [29]. We set $L_z = L_{\parallel} = L_{\hat{x}-\hat{y}} = L$ and add incommensurate potential $V \cos(2\pi\alpha m)$ along the $\hat{x} - \hat{y}$ direction, where m expresses the m -th layer along the $\hat{x} - \hat{y}$ direction. By using a similar method as the case in the absence of Fermi arc, we can obtain the following eigen-equations:

$$\begin{aligned}
 E_n \psi_{n,j,A} &= (-t_y e^{ik_{\parallel}/\sqrt{2}} - t_x e^{-ik_{\parallel}/\sqrt{2}}) \psi_{n,j-1,B} + [2t_z \cos k_z + V \cos(2\pi\alpha j)] \psi_{n,j,A} \\
 &\quad + (-t_y e^{-ik_{\parallel}/\sqrt{2}} + t_x e^{ik_{\parallel}/\sqrt{2}}) \psi_{n,j,B}, \\
 E_n \psi_{n,j,B} &= (-t_y e^{-ik_{\parallel}/\sqrt{2}} - t_x e^{ik_{\parallel}/\sqrt{2}}) \psi_{n,j+1,A} + (-t_y e^{ik_{\parallel}/\sqrt{2}} + t_x e^{-ik_{\parallel}/\sqrt{2}}) \psi_{n,j,A} \\
 &\quad + [-2t_z \cos k_z + V \cos(2\pi\alpha j)] \psi_{n,j,B},
 \end{aligned} \tag{9}$$

where k_{\parallel} belongs to $[-\pi/\sqrt{2}, \pi/\sqrt{2})$, k_z belongs to $[-\pi, \pi)$ and j expresses the j -th layer along the $\hat{x} - \hat{y}$ direction.

In Fig. 5(a), we display the energy dispersion of L -th and $(L+1)$ -th levels of the system without adding incommensurate potential ($V = 0$), and in Fig. 5(b) the spectrum as a function of k_{\parallel} by fixing $k_z = \frac{\pi}{2}$. It is shown that there exists Fermi arc connecting the Weyl points at $k_{\parallel} = \pm \frac{\pi}{2\sqrt{2}}$. When adding the incommensurate potential with the strength $V = 0.1$ to this system, the dispersion shapes of the L -th and $(L+1)$ -th levels change. As shown in Fig. 5(c), the Fermi arc corresponding to the

curve of $E = 0$ is destroyed, and the Weyl points are connected by curves of $E(k_{\parallel}, k_z) < 0$. For a half-filled system, the Fermi surface E_c moves down to $E_c < 0$, and the system enters into a metallic phase. Further increasing the incommensurate potential strength V , the dispersion shape of the L -th and $(L+1)$ -th levels change more dramatically as shown in Fig. 5(d), and there exists a bigger region with the $(L+1)$ -th level entering into the $E < 0$ region. Our results indicate that the WSM phase for the case without Fermi arcs are more robust against to the incommensurate potential than the case in the presence of Fermi arcs.

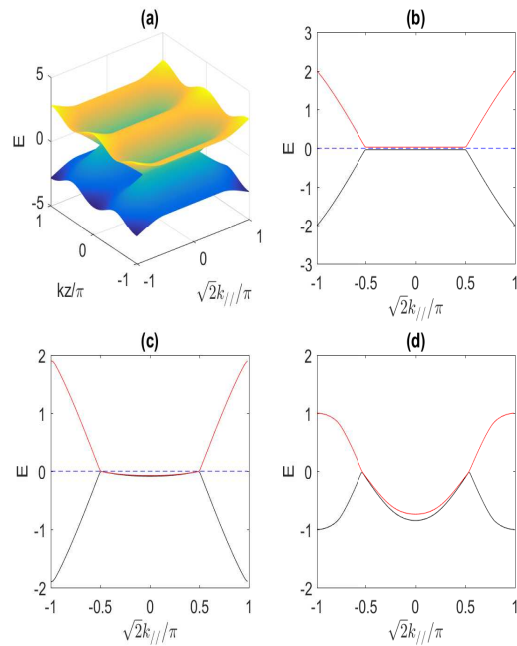


FIG. 5: (Color online) (a) Dispersions of the L -th and $(L+1)$ -th levels of the system with $V = 0$. (b)-(d) Dispersions of the L -th and $(L+1)$ -th levels as a function of $k_{||}$ with fixed $k_z = \frac{\pi}{2}$ for the system with (b) $V = 0$, (c) $V = 0.1$ and (d) $V = 1$. The dotted lines of (b) and (c) are the referenced line of $E = 0$. Other parameters are $t_x = t_y = t_z = 1$ and $L = 300$.

III. SUMMARY

In summary, we have studied the effect of incommensurate potential on WSM either in the absence or the presence of Fermi arcs. We show that the incommensurate potential plays obviously different roles in these two cases. For the system without Fermi arcs, the WSM is robust against the incommensurate potential. By calculating the DOS of the system, we show that the system enters into a metallic phase when the incommensurate potential strength exceeds a critical value, which is even bigger than the extended-localization transition point along the z direction. However, for the system in the presence of Fermi arcs, we show that the Fermi arcs are sensitive against the incommensurate potential, and the WSM is unstable even for a very small incommensurate potential.

Acknowledgments

The work is supported by the National Key Research and Development Program of China (2016YFA0300600), NSFC under Grants No. 11425419, No. 11374354 and No. 11174360, and the Strategic Priority Research Program (B) of the Chinese Academy of Sciences (No. XDB07020000).

-
- [1] M. Z Hassan and C. L. Kane, *Rev. Mod. Phys.* **82**, 3045 (2010).
- [2] X. L. Qi and S.-C. Zhang, *Rev. Mod. Phys.* **83**, 1057 (2011).
- [3] B.-J. Yang and N. Nagaosa, *Nat. Commun.* **5**, 4898 (2014).
- [4] C. Fang, Y. Chen, H.-Y. Kee, and L. Fu, *Phys. Rev. B* **92**, 081201 (2015); C. Fang, H. Weng, X. Dai, and Z. Fang, *C. Phys. B* **25** 117106 (2016).
- [5] S. Murakami, *New Journal of Physics* **9**, 356 (2007).
- [6] X. Wan, A. M. Turner, A. Vishwanath, and S. Y. Savrasov, *Phys. Rev. B* **83**, 205101 (2011).
- [7] A. A. Burkov and L. Balents, *Phys. Rev. Lett.* **107**, 127205 (2011); A. A. Burkov, M. D. Hook, and L. Balents, *Phys. Rev. B* **84**, 235126 (2011).
- [8] K.-Y. Yang, Y.-M. Lu, and Y. Ran, *Phys. Rev. B* **84**, 075129 (2011).
- [9] G. Xu, H. Weng, Z. Wang, X. Dai, and Z. Fang, *Phys. Rev. Lett.* **107**, 186806 (2011).
- [10] G. B. Halasz and L. Balents, *Phys. Rev. B* **85**, 035103 (2012).
- [11] S. M. Young, S. Zaheer, J. C. Y. Teo, C. L. Kane, E. J. Mele, and A. M. Rappe, *Phys. Rev. Lett.* **108**, 140405 (2012).
- [12] S.-M. Huang, S.-Y. Xu, I. Belopolski, C.-C. Lee, G. Chang, B. Wang, N. Alidoust, G. Bian, M. Neupane, C. Zhang, S. Jia, A. Bansil, H. Lin, and M. Z. Hasan, *Nature Comm.* **6**, 7373 (2015).
- [13] B. Q. Lv, N. Xu, H. M. Weng, J. Z. Ma, P. Richard, X. C. Huang, L. X. Zhao, G. F. Chen, C. E. Matt, F. Bisti, V. N. Strocov, J. Mesot, Z. Fang, X. Dai, T. Qian, M. Shiand, and H. Ding, *Nat. Phys.* **11**, 724 (2015).
- [14] S.-Y. Xu, I. Belopolski, N. Alidoust, M. Neupane, G. Bian, C. Zhang, R. Sankar, G. Chang, Z. Yuan, C.-C. Lee, S.-M. Huang, H. Zheng, J. Ma, D. S. Sanchez, B. Wang, A. Bansil, F. Chou, P. P. Shibayev, H. Lin, S. Jia, and M. Z. Hasan, *Science* **349**, 613 (2015).
- [15] S.-Y. Xu, N. Alidoust, I. Belopolski, Z. Yuan, G. Bian, T.-R. Chang, H. Zheng, V. N. Strocov, D. S. Sanchez, G. Chang, C. Zhang, D. Mou, Y. Wu, L. Huang, C.-C. Lee, S.-M. Huang, B.-K. Wang, A. Bansil, H.-T. Jeng, T. Neupert, A. Kaminski, H. Lin, S. Jia, and M. Z. Hasan, *Nat. Phys.* **11**, 748 (2015).
- [16] L. X. Yang, Z. K. Liu, Y. Sun, H. Peng, H. F. Yang, T. Zhang, B. Zhou, Y. Zhang, Y. F. Guo, M. Rahn, D. Prabhakaran, Z. Hussain, S.-K. Mo, C. Felser, B. Yan, and Y. L. Chen, *Nat. Phys.* **11**, 728 (2015).
- [17] Z. Huang, T. Das, A. V. Balatsky, and D. P. Arovos, *Phys. Rev. B* **87**, 155123 (2013).
- [18] Y. Ominato and M. Koshino, *Phys. Rev. B* **89**, 054202 (2014).
- [19] B. Sbierski, G. Pohl, E. J. Bergholtz, and P. W. Brouwer, *Phys. Rev. Lett.* **113**, 026602 (2014).
- [20] R. R. Biswas and S. Ryu, *Phys. Rev. B* **89**, 014205

- (2014).
- [21] C.-Z. Chen, J. Song, H. Jiang, Q.-F. Sun, Z. Wang, and X. C. Xie, *Phys. Rev. Lett.* **115**, 246603 (2015).
- [22] H. Shapourian and T. L. Hughes, *Phys. Rev. B* **93**, 075108 (2016).
- [23] S. Bera, J. D. Sau, and B. Roy, *Phys. Rev. B* **93**, 201302 (2016).
- [24] L. Radzihovsky, L. Radzihovsky, and V. Gurarie, *Phys. Rev. Lett.* **114**, 166601 (2015); S.V. Syzranov and L. Radzihovsky, arXiv:1609.05694.
- [25] K. Kobayashi, T. Ohtsuki, K.-I. Imura, and I. F. Herbut, *Phys. Rev. Lett.* **112**, 016402 (2014).
- [26] R. Nandkishore, D. A. Huse, and S. L. Sondhi, *Phys. Rev. B* **89**, 245110 (2014).
- [27] B. Roy and S. Das Sarma, *Phys. Rev. B* **90**, 241112 (2014).
- [28] J. H. Pixley, P. Goswami, and S. D. Sarma, *Phys. Rev. Lett.* **115**, 076601 (2015).
- [29] T. Dubčėk, C. J. Kennedy, L. Lu, W. Ketterle, M. Soljačić, and H. Buljan, *Phys. Rev. Lett.* **114**, 225301 (2015).
- [30] Z. Lan, N. Goldman, A. Bermudez, W. Lu, and P. Öhberg, *Phys. Rev. B* **84**, 165115 (2011).
- [31] J. H. Jiang, *Phys. Rev. A* **85**, 033640 (2012).
- [32] P. Delplace, J. Li, and D. Carpentier, *Europhys. Lett.* **97**, 67004 (2012).
- [33] D.-W. Zhang, S.-L. Zhu, and Z. D. Wang, *Phys. Rev. A* **92**, 013632 (2015).
- [34] W.-Y. He, S. Zhang, and K. T. Law, *Phys. Rev. A* **94**, 013606 (2016).
- [35] Y. Xu, F. Zhang and C. Zhang, *Phys. Rev. Lett.* **115**, 265304 (2015); Y. Xu and L. M. Duan, *Phys. Rev. A* **94**, 053619 (2016).
- [36] G. Roati et al., *Nature (London)* **453**, 895 (2008).
- [37] B. Deissler et al., *Nat. Phys.* **6**, 354 (2010).
- [38] S. Aubry and G. André, *Ann. Isr. Phys. Soc.* **3**, 133 (1980).
- [39] K. Machida and M. Fujita, *Phys. Rev. B* **34**, 7367 (1986).
- [40] T. Geisel R. Ketzmerick and G. Petschel, *Phys. Rev. Lett.* **66**,1651 (1991).
- [41] R. B. Diener, G. A. Georgakis, J. Zhong, M. Raizen, and Q. Niu, *Phys. Rev. A* **64**, 033416 (2001).
- [42] T. Roscilde, *Phys. Rev. A* **77**, 063605 (2008).
- [43] M. Albert and P. Leboeuf, *Phys. Rev. A* **81**,013614 (2010).
- [44] K. He, I. I. Satija, C. W. Clark, A. M. Rey, and M. Rigol, *Phys. Rev. A* **85**, 013617 (2012); C. Gramsch and M. Rigol, *Phys. Rev. A* **86**, 053615 (2012).
- [45] X. Cai, L.-J. Lang, S. Chen, and Y. Wang, *Phys. Rev. Lett.* **110**, 176403 (2013); X. Cai, S. Chen, and Y. Wang, *Phys. Rev. A* **81**, 023626 (2010).
- [46] Y. Lahini, R. Pugatch, F. Pozzi, M. Sorel, R. Morandotti, N. Davidson, and Y. Silberberg *Phys. Rev. Lett.* **103**, 013901 (2009).
- [47] D. J. Thouless, *Phys. Rep.* **13**, 93 (1974).
- [48] M. Schreiber, *J. Phys. C* **18**, 2493 (1985); Y. Hashimoto, K. Niizeki, and Y. Okabe, *J. Phys. A* **25**, 5211 (1992).
- [49] A. Weiße, G. Wellein, A. Alvermann, and H. Fehske, *Rev. Mod. Phys.* **78**, 275 (2006).